Three-dimensional surface profile measurement using a beam scanning chromatic confocal microscope

Byung Seon Chun, Kwangsoo Kim, and Daegab Gweon
Department of Mechanical Engineering, Korea Advanced Institute of Science and Technology, Guseong-dong, Yuseong-gu, Daejeon 305-701, Republic of Korea

In this research, chromatic confocal microscopy with transverse point beam scanning is constructed for three-dimensional surface measurement without longitudinal mechanical translation. In beam scanning chromatic confocal microscopy, the wavelength-to-depth relation and the lateral field of view should be determined considering the beam scanning angle. With the experimental results from a sample structure, the three-dimensional profile is reconstructed by relating the wavelength and scanning angle to the axial and the lateral coordinates. © *2009 American Institute of Physics.*
[DOI: 10.1063/1.3184023]

I. INTRODUCTION

The longitudinal depth scanning of confocal microscopy generally has been depending on the mechanical movement of the objective lens (OL) or the sample. A chromatic depth scan[1] was proposed to avoid the mechanical translation in confocal microscopy.[2] The chromatic depth scan was effectively realized by focusing the incident broadband light source to different axial positions through an intentionally generated longitudinal chromatic aberration. Since the different spectral components of the light source are focused onto the planes at different depth levels, the polychromatic illumination and the spectrum analysis of the light reflected from the sample can possibly work as an alternative method for mechanical depth scanning.

Figure 1 shows a schematic diagram of chromatic confocal microscopy. When a polychromatic point light source illuminates, the rays of different wavelengths are focused onto different focal points along the optical axis by longitudinal chromatic aberration. Following the ray of λ_d, of which the corresponding focal point is precisely on the sample surface, the reflected ray of λ_d will pass through the pinhole. On the other hand, following the ray of λ_1 or λ_n, which is focused at a distance from the sample surface, the spot size formed on the pinhole plane by the reflected ray of λ_1 or λ_n is broadened and out-of-focus rejection takes place by the pinhole aperture. Thus, by reading the wavelength of the most intense signal in the power spectrum after the pinhole, the depth position of the sample surface can be found.

The range of the depth scan, which is a variation in the focal length, is determined by the bandwidth of the light source and the dispersive properties of the lens. The axial chromatic dispersion can be generated either by the refractive lens or by the diffractive lens.[3] To achieve a larger scanning range and higher signal-to-noise ratio, a broadband source, such as a xenon arc lamp and a supercontinuum laser, can be used as a light source for chromatic confocal microscopy.[4–6]

To obtain three-dimensional surface profile, transverse scanning should be accompanied with depth scanning. The implementation of transverse scanning can be categorized as stage scanning, moving pinhole scanning, and moving beam scanning as in confocal microscopy.[7] Stage scanning is a form of using a stationary beam and a moving object. It is conceptually simple and technically accurate as diffraction limited optics can be easily implemented for the on-axis focus. The drawback of stage scanning is that its imaging speed is very slow and it is difficult to implement when the samples are large and heavy. Moving pinhole scanning is conducted by changing the position of the source and detection conjugate points in an image plane. A rotating Nipkow disk using the parallel pinhole array to scan the transverse plane is a good example of moving pinhole scanning. It can greatly improve the imaging speed; however, it has the disadvantages of low light efficiency and high backscatter noise.

Moving beam scanning is done by changing the incident angle of the beam at a pupil plane with devices such as galvanometer mirrors, rotating polygonal mirrors, acousto-optic deflectors, etc. It is fast enough up to or more than video-rate with high beam quality and high light efficiency, although the drawback of this type of scanning method is that the instruments are relatively complex.

There was some research on the chromatic confocal microscopy combined with the lateral scanning. Lin *et al.*[8] incorporated a slit-scan confocal technique into a chromatic confocal microscope. This system was designed to measure a two-dimensional position (*x* and *z*) on the sample surface, and an additional mechanical stage scanning was necessary to complete three-dimensional measurements. Tiziani *et al.*[9] applied the chromatic depth scanning method to the confocal microscope with a rotating Nipkow disk. They determined the height by taking a color image of a sample and by the appropriate evaluation of its color tone. It is a kind of chromatic method for confocal measurement, but is somewhat different from the wavelength-to-depth codification method, as described in Fig. 1. Cha *et al.*[10] used a digital micromirror device (DMD) for transverse scanning in their chromatic confocal microscope. The DMD scanning in a confocal mi-
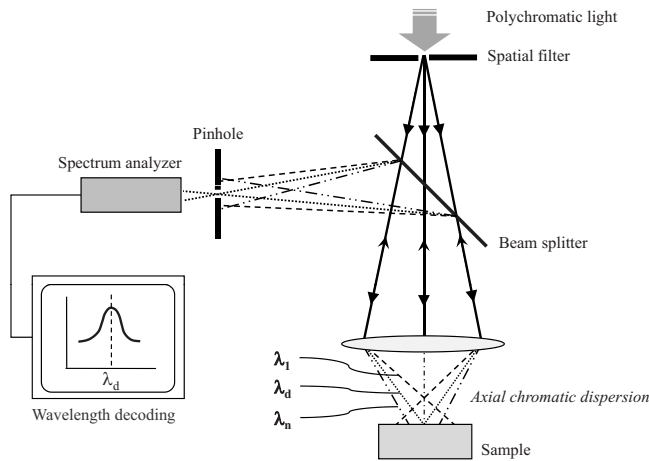
FIG. 1. Principle of chromatic confocal microscopy.

croscope is theoretically similar to the scanning by a Nipkow disk, which is a kind of moving pinhole scanning, and also has the disadvantage of low light efficiency.

Among the three types of transverse scanning methods previously mentioned, the incorporation of the chromatic depth scanning and the moving beam scanning for three-dimensional surface measurement has not been reported yet. This moving beam scanning or beam scanning is popularly used for commercial confocal microscopes due to its benefit of high efficiency and relatively high measurement speed.

In this experiment, a beam scanning chromatic confocal microscope was constructed with galvanometer mirrors, and the effect of transverse point beam scanning in chromatic confocal microscopy was investigated.

II. EXPERIMENTAL SETUP

Figure 2 shows the schematic layout of the beam scanning chromatic confocal microscope. The illumination system is composed of a broadband xenon lamp (Perkin Elmer, PE300BF) with a parabolic mirror focusing on the pinhole (PH1). The radius of the pinhole (PH1) is 5 μm, and it was regarded as a broadband point light source. The working range of the wavelength used in this experiment is between
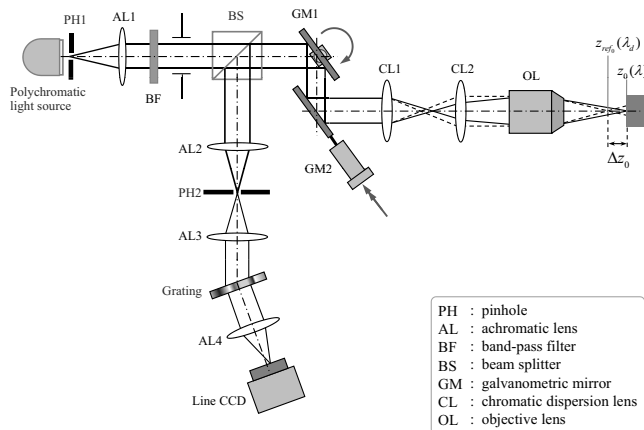

FIG. 2. Schematic diagram of a beam scanning chromatic confocal microscope.

500 and 600 nm, and the design wavelength (λ_d) is 550 nm, the central wavelength in this working range.

A broadband point light source is collimated by an achromatic 10× OL (AL1). The band-pass filter (BF) (Edmund Optics, 46-433) is used to improve the signal-to-noise ratio of the detection beam by cutting off the wavelengths out of the working range. Passing through the beam splitter (BS) (Edmund Optics, 45-852), the heading direction of the collimated beam is properly controlled by two-axis galvanometer mirrors (GM1 and GM2) (Cambridge Technologies, 6230H) for lateral scans before the chromatic dispersion generating optics composed of a pair of singlet lenses (CL1 and CL2; CVI Laser, PLCX-25.4-45.7-SF11). This pair of singlet lenses is composed of two SF11 planoconvex lenses. The radius of curved surface is 45.7 mm, and the lens thickness is 3.8 mm. The distance between the second surface of lens CL1 and the first surface of lens CL2 is 111.2 mm, which constitutes the one-to-one afocal system at the design wavelength λ_d. This pair of lenses also plays the role of relay optics between an OL and two-axis galvanometer mirrors which are closely aligned. The distance between the centers of galvanometer mirrors is 10 mm, and the distance between the second galvanometer GM2 and the first surface of lens CL1 is 50.6 mm.

After the pair of singlet lenses, the converging angle of the beam incident to the OL varies by wavelength. The converging angle decreases as the wavelength becomes longer. The beam has a maximum converging angle at the shortest wavelength, 0 at the design wavelength λ_d, and a maximum diverging angle at the longest wavelength in the working range. This convergence determines the longitudinal position of the focus formed by the OL. The microscope OL used in this experiment is an Olympus 20× lens with a focal distance of 9 mm and a numerical aperture of 0.46. The distance between the second surface of lens CL2 and the objective is 55.6 mm.

The light reflected from the sample turns back to the BS. Then it is reflected and focused on the detection pinhole (PH2) aperture by the achromatic lens (AL2). The nominal focal distance of the achromatic lens (AL2) is 45 mm, and the radius of the pinhole (PH2) is 2.5 μm. As the diameter of the beam incident to this achromatic lens (AL2) is 8 mm, which is the same size as the rear aperture of the OL, the radius of the pinhole (PH2) in optical coordinate[11] ($2\pi r NA/\lambda$) is 2.53 at the design wavelength. The pinhole size in optical coordinate is dependent on the wavelength. Ruprecht et al.[12] reported that the variation in the full width at half maximum (FWHM) value of chromatic confocal microscopy due to its wavelength dependence is only within 1% in the interval from 0.71 to 1.13 of normalized wavelength. The wavelength range used in our system is from 0.91 to 1.09 if expressed by normalized wavelength.

As the focal points in object space are longitudinally distributed by wavelength, only the light of a specific wavelength corresponding to the focal point on the sample surface passes through the pinhole. The three conjugated points of this system are the polychromatic point light source, the focal point for a determined wavelength, and the detection pinhole. The depth information of the sample can be obtained

by reading the most intense spectral component after the pinhole (PH2). To analyze the spectrum of the reflected signal after the pinhole (PH2), the light passing through the pinhole is collimated by an achromatic lens (AL3), which is the same as lens AL2, and laterally dispersed by a grating (Wasatch Photonics, 600 lines/mm). The number of resolvable points by the grating for the first diffraction order[13] is calculated by the equation

$$N_r = \frac{D}{\cos \theta_d} \frac{f \Delta \lambda}{\lambda_d}, \tag{1}$$

where D is an input beam diameter, θ_d is the angle of diffraction, f is the spatial frequency of the grating, and $\Delta \lambda$ is a spectral bandwidth. In this system, for the center wavelength of 550 nm, a bandwidth of 100 nm, an input beam diameter of 8 mm, a grating line frequency of 600 lines/mm, and the diffraction angle of 9.5°, 884 points are resolved.

The laterally dispersed light is imaged on a line charge-coupled device (CCD) camera (Dalsa, S3–20–01K40) by an achromatic lens (AL4) with a nominal focal length of 173.6 mm. Each pixel of the line CCD corresponds to the specific wavelength.

III. SYSTEM CHARACTERIZATION AND RESULTS

The focal position determined by the light of design wavelength λ_d is the reference position $[z_{\text{ref}}(\lambda_d)]$, and the shift of the focus from the reference position is a function of λ, defined as

$$\Delta z_0 = z_{\text{ref}_0}(\lambda_d) - z_0(\lambda), \tag{2}$$

where $z(\lambda)$ is a longitudinal focal distance of a determined wavelength. The 0 subscript is added to indicate that the scanning angles are set to 0.

This relation of wavelength to the focal shift at the optical axis can be calculated from an equation[6]

$$\Delta z_0 = \frac{\Delta n}{(n-1)} (F_{\text{CL1}} + F_{\text{CL2}}) \frac{F_{\text{OL}}^2}{F_{\text{CL2}}^2}, \tag{3}$$

where F_{CL1}, F_{CL2}, and F_{OL} are the focal lengths of the singlet lenses (CL1 and CL2) and the OL depicted in Fig. 2. As the refractive index n can be expressed as a function of wavelength by the Sellmeier equation,[14] the wavelength-to-depth relation can be obtained by Eq. (3).

The wavelength-to-depth relation can also be found by *ray tracing* method.[15] Ray tracing method is fundamentally the expansion of the Snell's law applied to the rays on each point of the spherical surface. Once the radii of lens surfaces and the refractive indices are known, the position and the direction of rays exit from the next surface can be calculated by using those from the previous surface. By applying this method to the bundle of rays incident to the first surface, the position of final focusing spot can be found.

The wavelength-to-depth relation at the optical axis is as plotted in Fig. 3. The solid line is the result of numerical simulation of ray tracing, the dashed line is the result of calculation by Eq. (3), and the rectangular dots are the experimental result. In the numerical simulation of ray tracing, the surface and arrangement data of galvanometer mirrors, a
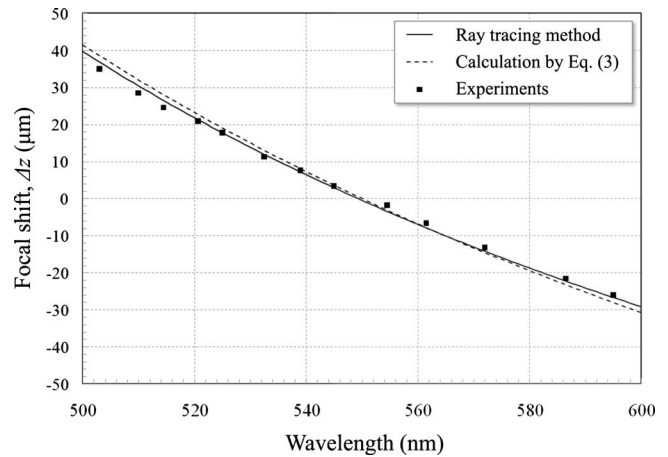

FIG. 3. Plot of wavelength-to-depth codification at 0 scanning angle.

pair of singlet lenses, and an OL were used. It was assumed that the OL obeys the sine condition perfectly as the actual OL data were not available. The chromatic depth scan range in the wavelength from 500 to 600 nm is about 69 μm.

When the beam is transversely scanned by galvanometer mirrors, the incident beam is not along the optical axis, and Eq. (3) cannot reflect this deviation. However, even oblique or skew rays can be traced by ray tracing method. As an example, Fig. 4(a) shows a surface plot of the determined wavelengths experimentally obtained by scanning a flat mirror at a fixed position. When the flat surface is scanned, the determined wavelength varies with the change of scanning angle. This variation can be figured out numerically by ray tracing method. Figure 4(b) shows the cross-sectional profile of Fig. 4(a), compared with the theoretical prediction by ray tracing. The change in the determined wavelength due to the scanning angle is plotted in Fig. 5 at some specific positions. It can be seen that the difference of more than 2 μm would be misread if this variation is not considered.

In the beam scanning chromatic confocal microscope, the wavelength-to-depth relations at all scanning angle positions should be found to reconstruct the three-dimensional image. Thus, Eq. (2) should be extended as a function of the scanning angles as well.

$$\Delta z(\alpha_x, \alpha_y) = z_{\text{ref}}(\lambda_d; \alpha_x, \alpha_y) - z(\lambda; \alpha_x, \alpha_y), \tag{4}$$

where α_x and α_y are scanning angles in transverse x and y directions, respectively.

The lateral field of view in conventional confocal microscopy remains constant during plane-by-plane imaging because the depth scanning is conducted by translating the OL or the sample while the focal plane itself remains same. However, in chromatic confocal microscopy, the lateral field of view covered by the same scanning angle changes with the wavelength or the position of the focal plane correspondent to the wavelength.

The lateral field of view is measured with a microruler (Olympus, objective micrometer). The data were obtained at the different longitudinal positions of a microruler with the same beam scanning angle. Figure 6 shows the comparison of raw data when the microruler is positioned at $\Delta z = +35$ μm, and $\Delta z = -26$ μm, of which the correspondent
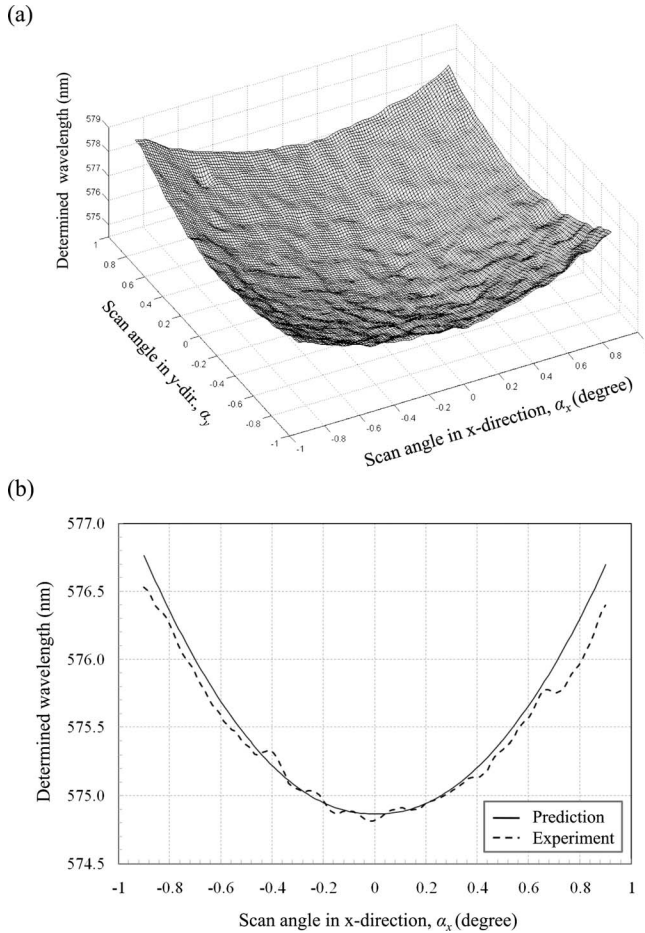
(a)

(b)

FIG. 4. (a) Surface plot of experimentally determined wavelength for a flat mirror positioned at $\Delta z = -15$ μm, and (b) its cross-sectional profile cut by $\alpha_y = 0°$.

wavelength on the optical axis is measured as 503 and 595 nm, respectively. For the distance of 200 μm in the microruler, 18 pixels are allotted more when the microruler is positioned at $\Delta z = -26$ μm. As the number of pixels constituting an image is the same regardless of the position of the microruler, less field of view is made when the microruler is positioned at $\Delta z = -26$ μm than at $\Delta z = +35$ μm.
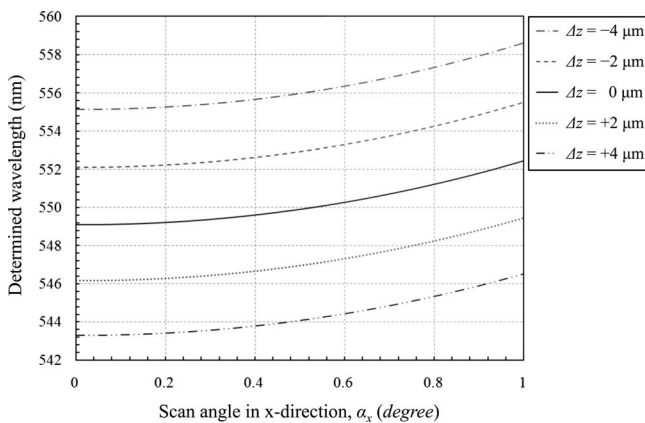

FIG. 5. Plot of scanning angle vs determined wavelength for the fixed flat plane at some specific positions. Results of numerical simulation by ray tracing with $\alpha_y = 0°$.
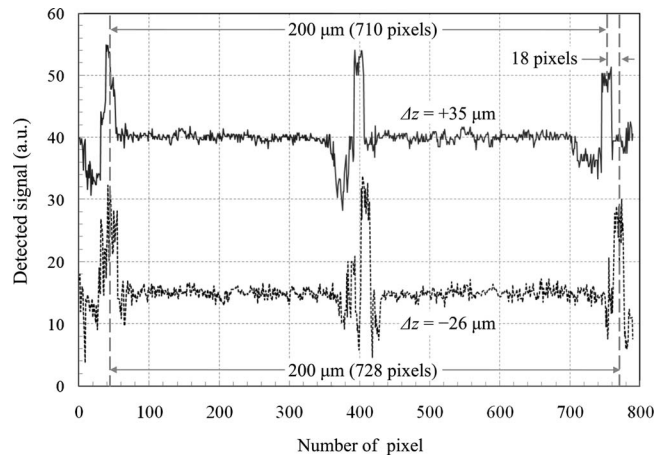

FIG. 6. Difference in the lateral field of view when a microruler is positioned at $\Delta z = +35$ μm (solid line) and $\Delta z = -26$ μm (dotted line).

In Fig. 7, the lateral field of view covered by the same scanning angle (from $-0.9°$ to $+0.9°$) is plotted with respect to the longitudinal positions of the microruler.

From this point of view, the longitudinal position of the sample surface should be considered to determine the lateral dimension of a target sample. The lateral field of view is defined as a function of not only the scanning angle, but also the longitudinal position of an imaging point on the sample surface. As the longitudinal position is related to the wavelength, the variation in the lateral field of view is also a function of wavelength and scanning angles

$$\Delta l(\alpha_x, \alpha_y) = l_{\text{ref}}(\lambda_d; \alpha_x, \alpha_y) - l(\lambda; \alpha_x, \alpha_y), \qquad (5)$$

where $l(\lambda; \alpha_x, \alpha_y)$ is a position coordinate in the transverse plane when the determined wavelength is λ with scanning angles of α_x and α_y. $l_{\text{ref}}(\lambda_d; \alpha_x, \alpha_y)$ is a reference position coordinate.

It is worth noting that with the assumption that the OL obeys the sine condition, the different plot is made by ray tracing method, i.e., the slope of the curve becomes opposite, as shown in Fig. 7. Thus, the calibration of lateral field of view should be made from experiments unless the OL data are available.
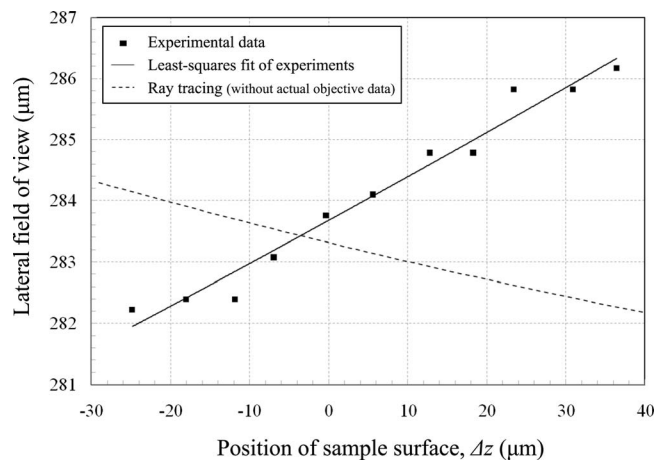

FIG. 7. Plot of depth position vs width of lateral field of view. By experiments, the lateral field of view increases as the sample is moving toward the OL.
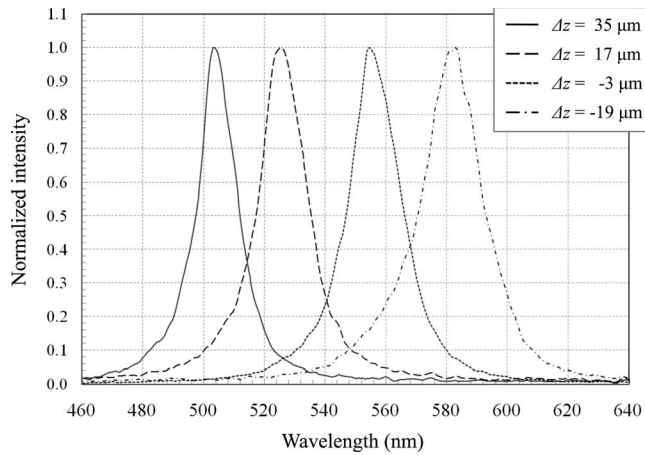
FIG. 8. Normalized spectral response measured at for four positions of a flat mirror.

The relations of Eq. (4) and Eq. (5) can be established by ray tracing or experimentation. As the lens data of a commercial OL are generally not available, the experimental calibration is necessary. Once the system is constructed, Eq. (4) can be established experimentally by recording the dominant wavelength reflected from a target mirror surface at each scanning angular position and repeating it at the various positions of a mirror surface. Equation (5) can be established experimentally by measuring the field of view with something such as a microruler at the various longitudinal positions, and by relating the scanning angle and the longitudinal position to the correspondent lateral position.

Then, when we measure the determined wavelength λ at each scanning position, which corresponds to one pixel of an image, we can identify the axial coordinate from Eq. (4) and the lateral coordinate from Eq. (5), and this will construct the three-dimensional surface profile.

The depth discrimination power of a confocal microscope is often represented by the FWHM. For the conventional confocal microscope, the FWHM is measured by moving a mirror through the focal plane and plotting the intensity of detected signal as a function of z. For the chromatic confocal microscope, the FWHM of the spectral response is measured for the mirror fixed at a position inside the depth scanning range.[3,5] Figure 8 shows the spectral responses measured at four different positions of a mirror, and Fig. 9(a) shows the plot of the spectral FWHM experimentally measured with respect to the position of a mirror. This spectral FWHM can be transformed to the correspondent axial distance by the wavelength-to-depth codification of Fig. 3. As the slope of the curve ($\Delta z/\Delta \lambda$) becomes slower with the increase in wavelength, the descending trend shown in Fig. 9(a) is relieved when it is transformed to the axial FWHM. The axial FWHM varies from 11.15 to 14.6 μm over the depth scanning range as in Fig. 9(b).

Figure 10 shows the intensity FWHM for the single wavelength, which is obtained by measuring the intensity at only one pixel of line CCD corresponding to the design wavelength while physically translating the mirror in axial direction. If the intensity at only one pixel is measured, this system can be regarded as a monochromatic confocal system
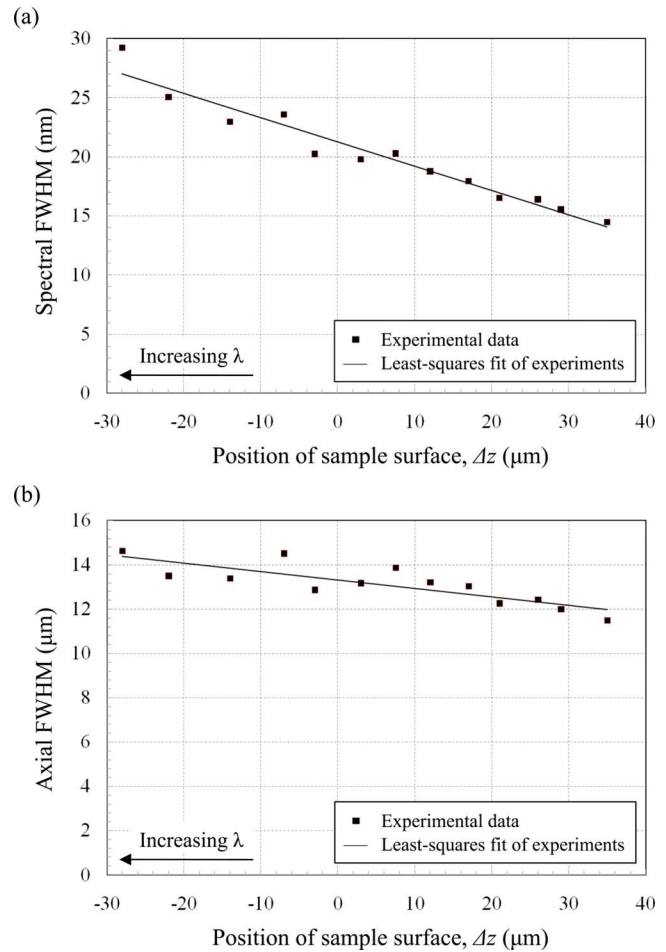

FIG. 9. (Color online) Plot of depth position vs (a) spectral FWHM, and (b) axial FWHM.

using the light of wavelength correspondent to the pixel number. The intensity FWHM is measured as 8.7 μm at the design wavelength. The axial FWHM measured by the spectral response as in Fig. 9(b) showed some degradation compared with the intensity FWHM for the single wavelength. It is presumed that this difference is caused by the nonuniformity of power spectrum of a light source.
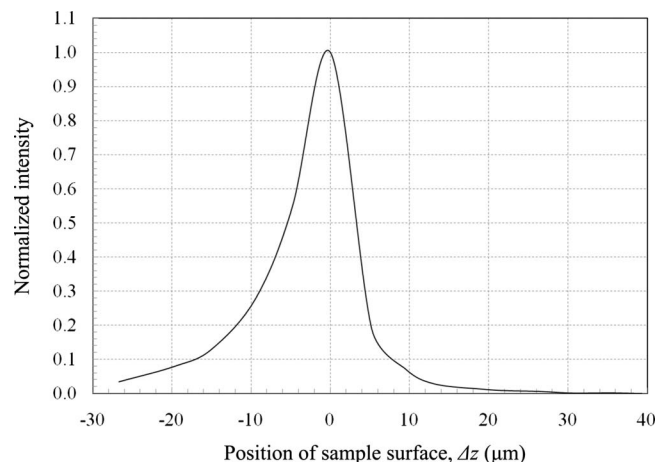

FIG. 10. Normalized intensity FWHM for the single design wavelength. Normalized intensity at one pixel of line CCD is measured with physically translating the mirror in axial direction.
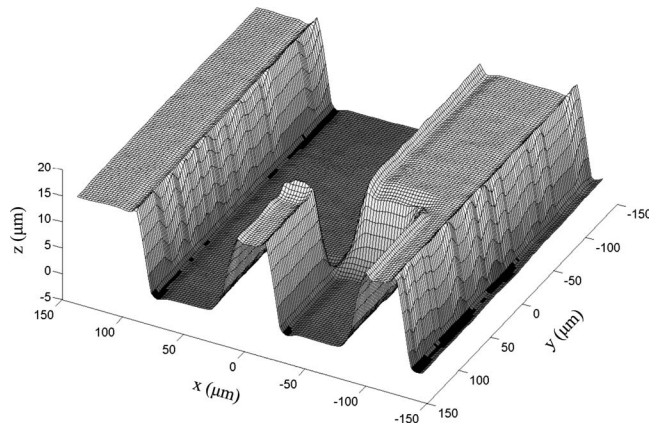
FIG. 11. Three-dimensionally reconstructed surface image of the height standard sample.

FIG. 12. Plot of cross-sectional profile cut by (a) $y=0$ μm plane and (b) $y=100$ μm plane.

Although the FWHM is an important characterization of a confocal microscope, it does not define the actual limit of depth resolution of the chromatic confocal microscope. If a center-of-mass technique is used to find depth position, the depth resolution can be much improved beyond that defined by the FWHM.[8] Cha *et al.*[10] defined the depth resolution of a chromatic confocal microscope by a standard deviation from the curve fit of wavelength-to-depth coding data. The axial resolution is also related to the pixel resolution of the line CCD (Ref. [6]) and the number of resolvable points of a diffraction grating.

As the number of pixels we use for the working wavelength range is 755 pixels, and the number of resolvable points is calculated as 884 points from Eq. [(1)], the resolution from this viewpoint is restricted by the pixel resolution of the line CCD. The pixel resolution for the longitudinal direction is 0.21 μm, obtained from dividing the correspondent height range of 69 μm by the number of pixel and multiplying it by a Nyquist sampling factor of 2.3. However, as this pixel resolution is less than the standard deviation experimentally measured as 0.72 μm from the curve fit of wavelength-to-depth codification, we concluded the depth resolution of our system is 0.72 μm.

The lateral resolution is determined according to the Rayleigh equation. As the working wavelength changes from 500 to 600 nm, its lateral resolutions change from 0.66 to 0.80 μm, respectively. The field of view at design wavelength is 284×284 μm^2.

The height standard sample (VLSI, SHS-14.5QC) was measured with our beam scanning chromatic confocal microscope. The three-dimensional information was gathered by scanning the two-axis galvanometer mirrors without the mechanical longitudinal motion. The three-dimensional surface profile was reconstructed by relating the wavelength and scanning angles to the height and the lateral coordinates. Figure 11 shows the three-dimensional reconstructed image, and its cross-sectional profile is shown in Fig. 12.

The actual step height of this standard sample is reported as 14.494 ± 0.087 μm, which is traceable by the National Institute of Standards and Technology. The lateral period of this pattern was measured as 200 μm by a commercial laser

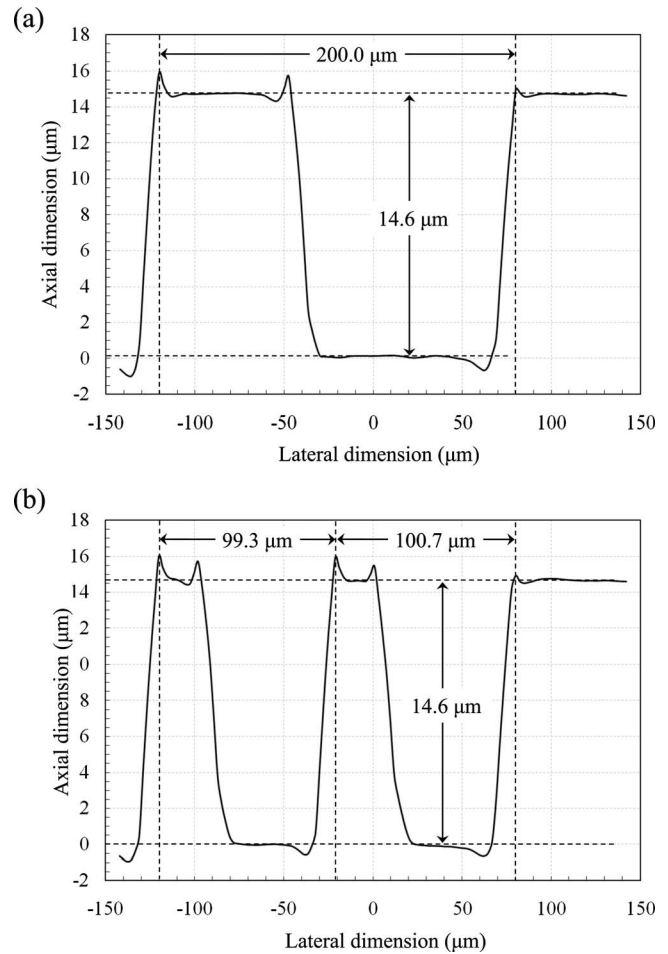confocal microscope. The measurement of the height and the period with our system, as shown in Figs. 12(a) and 12(b), shows a good match with the actual value.

IV. CONCLUSION

The chromatic depth scanning confocal microscopy is the promising technique for high speed three-dimensional measurement as it does not require the mechanical translation in axial direction. We constructed the beam scanning chromatic confocal microscope using the galvanometric transverse scanning mechanism, which is popularly used in commercial laser scanning confocal microscopes due to its benefit of high efficiency and relatively high speed.

When the chromatic confocal microscope is incorporated with the beam scanning mechanism, the wavelength-to-depth codification of chromatic scan should be found with respect to the beam scanning angular position. As the lateral field determined by the beam scanning angle varies with the depth position, it should be compensated to reconstruct the correct three-dimensional profile.

As the measurement speed of the chromatic confocal microscope is practically limited not by the transverse scanning speed but by the spectral detection speed, the moving pinhole scanning method cannot be operated at its full speed.

By applying the beam scanning method to the chromatic confocal microscope, it can be operated with high light efficiency and considerably high speed as well.

Enhancing the uniformity of a broadband light source would increase the depth discrimination power. The lens design of chromatic dispersion generating optics, which maximizes the longitudinal chromatic aberration and minimizes the other aberrations in the working range of wavelength, would allow more field angle resulting in the larger field of view.

[1] G. Molesini, G. Pedrini, P. Poggi, and F. Quercioli, Opt. Commun. **49**, 229 (1984).

[2] M. A. Browne, O. Akinyemi, and A. Boyde, Scanning **14**, 145 (1992).

[3] S. L. Dobson, P.-C. Sun, and Y. Fainman, Appl. Opt. **36**, 4744 (1997).

[4] K. Shi, P. Li, S. Yin, and Z. Liu, Opt. Express **12**, 2096 (2004).

[5] J. Garzón, J. Meneses, G. Tribillon, T. Gharbi, and A. Plata, J. Opt. A, Pure Appl. Opt. **6**, 544 (2004).

[6] K. Shi, S. H. Nam, P. Li, S. Yin, and Z. Liu, Opt. Commun. **263**, 156 (2006).

[7] R. H. Webb, Rep. Prog. Phys. **59**, 427 (1996).

[8] P. C. Lin, P.-C. Sun, L. Zhu, and Y. Fainman, Appl. Opt. **37**, 6764 (1998).

[9] H. J. Tiziani and H.-M. Uhde, Appl. Opt. **33**, 1838 (1994).

[10] S. Cha, P. C. Lin, L. Zhu, P.-C. Sun, and Y. Fainman, Appl. Opt. **39**, 2605 (2000).

[11] T. Wilson and A. R. Carlini, Opt. Lett. **12**, 227 (1987).

[12] A. K. Ruprecht, T. F. Wiesendanger, and H. J. Tiziani, Opt. Lett. **29**, 2130 (2004).

[13] G. J. Tearney, R. H. Webb, and B. E. Bouma, Opt. Lett. **23**, 1152 (1998).

[14] W. J. Smith, in *Modern Optical Engineering*, 2nd ed., edited by H. McGraw, (McGraw-Hill, New York, 1990).

[15] M. Born and E. Wolf, *Principle of Optics*, 6th ed. (Pergamon, New York, 1980).